Opportunistic Energy Harvesting and Energy-Based Opportunistic Spectrum Access in Cognitive Radio Networks

Yuanyuan Yao(✉), Xiaoshi Song, Changchuan Yin, and Sai Huang

Beijing Key Laboratory of Network System Architecture and Convergence, Beijing University of Posts and Telecommunications, Beijing, China
{yyyao,songxiaoshi,ccyin,huangsai}@bupt.edu.cn

Abstract. The performance of large-scale cognitive radio (CR) networks with secondary users self-sustained by opportunistically harvesting radio-frequency (RF) energy from nearby primary transmissions is investigated. Using an advanced RF energy harvester, a secondary user is assumed to be able to collect ambient primary RF energy as long as it lies inside the harvesting zone of an active primary transmitter (PT). A variable power (VP) transmission mode is proposed, and a simple energy-based opportunistic spectrum access (OSA) strategy is considered, under which a secondary transmitter (ST) is allowed to transmit if its harvested energy is larger than a predefined transmission threshold and it is outside the guard zones of all active PTs. The transmission probability of the STs is derived. The coverage probabilities and the throughputs of the primary and the secondary networks, respectively, are characterized. The throughput can be increased by as much as 29%. Simulation results are provided to validate our analysis.

Keywords: Cognitive radio · Energy-based opportunistic spectrum access · Energy harvesting · Stochastic geometry · Transmit threshold

1 Introduction

Radio frequency (RF) energy harvesting holds promise for generating a small amount of electrical power to drive the circuits in wireless devices. Communication devices often have omni-directional antennas that propagate RF energy in all directions, and some of this power can be harvested to augment/replenish battery power in networks constituted of low-power devices such as wireless sensors [1].

Stochastic geometry theory [2] has been widely applied in the study of large-scale cognitive radio (CR) networks with energy harvesting. In [3], Dhillon *et al.*

This work was supported in part by the NSFC under Grants 61271257 and 61328102, the National Research Foundation for the Doctoral Program of Higher Education of China under Grant 20120005110007.

M. Weichold et al. (Eds.): CROWNCOM 2015, LNICST 156, pp. 187–198, 2015.
DOI: 10.1007/978-3-319-24540-9_15

developed a tractable model for K-tier heterogeneous cellular networks, where each base station is powered solely by a self-contained energy harvesting module. In [4], equipped with an advanced RF energy harvester, a secondary transmitter (ST) is assumed to be able to collect ambient RF energy from its nearest active primary transmitter (PT). However, it is assumed that the batteries of STs must be fully charged before their transmission, i.e., all the STs transmit with the same power, which theoretically limits the network capacity and in practise would result in a low level of convenience.

In general, since the energy arrivals are random and the energy storage capacities are finite, variable power (VP) transmission mode is more realistic. In this paper, we investigate the performance of a large-scale CR network with secondary users self-sustained by opportunistically harvesting RF energy from the primary transmissions. An energy-based OSA strategy is considered, under which STs use VP for transmission. Time is assumed to be slotted. In each time slot, a ST is considered to collect ambient primary RF energy if it lies inside the harvesting zone of an active PT, or start to transmit if its harvested energy is larger than a predefined transmission threshold and it is outside the guard zones of all active PTs, or be idle otherwise. By applying tools from stochastic geometry, the transmission probability of the STs is derived. Based on the results, we then characterize the coverage probabilities and throughputs of the primary and the secondary networks, respectively. Note that compared with [4], our proposed energy-based OSA protocol does not require the candidate STs to be fully charged before their transmissions, i.e., STs use VP for transmission, which considerably improves the reliability and stability of the CR network.

The remainder of this paper is organized as follows. The system model and performance metrics are introduced in Section 2. Section 3 investigates the transmit opportunity for the STs. The coverage performance of the primary and the secondary networks are studied in Section 4. Section 5 analyzes the primary and the secondary network throughputs, respectively. Simulation results are presented in Section 6. Finally, we conclude the paper in Section 7.

2 System Model

2.1 Network Model

We consider a large-scale CR network which consists of two mobile ad hoc networks, i.e., the primary network and the secondary network, on $\mathbb{R}^2$. The locations of the PTs and STs are assumed to follow two independent homogeneous Poisson point processes (HPPPs) with density μ_p' and μ_s, respectively, where we assume $\mu_p' \ll \mu_s$. For each PT, its associated primary receiver (PR) is located at a distance of d_p away in a random direction. Similarly, for each ST, its associated secondary receiver (SR) is located at a distance of d_s away in a random direction. We further assume that PTs use the same power P_p for data transmissions and STs use VP for data transmissions. The maximum transmit power of STs is P_s, which occurs when the batteries of STs are fully charged. In addition, $P_p \gg P_s$.

Time is partitioned into slots with unit duration. In each time slot, the PTs employ an Aloha type of medium access control (MAC) protocol and make independent decisions to access the spectrum with probability p_p. Then, according to the coloring theorem [2], the locations of the active PTs follow a HPPP with density $\mu_p = p_p\mu'_p$ [5]. We further denote $\Phi_p = \{X\}$ and $\Phi_s = \{Y\}$ as the point processes formed by the active PTs and STs, respectively, where X and Y denotes the coordinates of the PTs and STs, respectively.

Each PT is assumed to be associated with a guard zone to protect its intended receiver from STs' interference, and at the same time delivers RF energy to STs located in its harvesting zone. For the secondary network, a VP transmission mode is proposed and an energy-based OSA strategy is considered, under which a ST is allowed to transmit if its harvested energy is larger than a predefined transmission threshold, which is given by βP_s, and it is outside the guard zones of all active PTs, where β, $0 < \beta \leq 1$, is the transmission threshold coefficient. Note that the special case with $\beta = 1$ was considered in [4]. For simplicity, we refer to "active PTs" as PTs in the sequel.

The propagation channel is modeled as the combination of small-scale Rayleigh fading and large-scale path-loss given by $g(r) = hr^{-\alpha}$, where h denotes the exponentially distributed power coefficient with unit mean, r denotes the propagation distance, and $\alpha > 2$ is the path-loss exponent.

2.2 Energy Harvesting Model

The RF harvester in the ST is equipped with a power conversion circuit, which can transform the received electromagnetic wave from the PTs into direct-current (DC) power; as such the secondary network can utilize the harvested energy from RF signals to augment/replenish their power sources. The input power needs to be larger than a predesigned threshold, which is given by $P_p r_h^{-\alpha}$, for the circuit to harvest RF energy efficiently. r_h is defined as the radius of a disk which is called the harvesting zone and is centered at each PT, that is to say, a ST could harvest RF energy from its nearest PT provided it is inside the harvesting zone. Otherwise, the power received by a ST outside any harvesting zone is too small to activate the energy harvesting circuit, and thus is assumed negligible. We denote the probability that ST lies in a harvesting zone as p_h. Similar as in [4], we assume that the harvesting zones of different PTs do not overlap at most time. Thus we have

$$p_h = 1 - e^{-\pi r_h^2 \mu_p}. \tag{1}$$

Let η $(0 < \eta < 1)$ denote the harvesting efficiency, the distance between a ST and its nearest PT be given by D and $D \leq r_h$. Then, the average energy harvested by a ST in one slot can be obtained as $\eta P_p D^{-\alpha}$. Note that the harvested power has been averaged over the channel short-term fading within a slot.

2.3 ST Transmit Model

The STs access the spectrum of the primary network and cause interference to PRs. To protect the primary transmissions, the STs are prevented from transmitting when they lie in any of the guard zones, modeled as disks with a fixed radius r_g ($r_g \gg r_h$) centered at each PT. With the energy-based OSA strategy, the STs using the VP transmission mode are allowed to transmit under the following condition. The STs should be located outside any of the guard zones (the probability is denoted as p_g) and the power of STs should be larger than the transmission threshold βP_s (the probability is p_c). When the battery is charged larger than the transmission threshold and if it is outside all the guard zones, the ST will transmit all the stored energy in the next slot. Note that in our model the battery power level of every active ST is in the range $[\beta P_s, P_s]$, which is different from the model in [4]. Moreover, the point processes formed by the PTs change independently over different slots. Therefore, the events that a ST has been charged to the transmission threshold in one slot, and that it is outside all the guard zones in the next slot are independent. Accordingly, the transmit probability of the STs denoted by p_t is obtained by

$$p_t = p_c p_g. \tag{2}$$

The calculation of p_c will be discussed in Section 3, and p_g can be given similarly to p_h, as

$$p_g = e^{-\pi r_g^2 \mu_p}. \tag{3}$$

2.4 Performance Metric

In addition to transmission probability, two more performance metrics are studied in this paper, coverage probability and network throughput, which are specified as follows.

Coverage Probability. The coverage probability means the transmission non-outage probability, which is defined as the probability that a PR/SR decodes the received data packets successfully from its corresponding PT/ST. Specifically, given the signal-to-interference ratio (SIR), and a corresponding SIR target, denoted by θ, the coverage probability in the network is defined as $\tau = \Pr\{\text{SIR} \geq \theta\}$.

Network Throughput. The throughput of the primary network or the secondary network is the maximum rate the system can achieve with successful primary/secondary transmissions. Assume that the active PTs/STs follow a HPPP with average density μ. Consequently, the network throughput is given by $C = \mu\tau \log(1 + \theta)$.

3 Transmission Probability in Secondary Network

From (2), it can be observed that p_t depends on p_c and p_g. In this section, we first derive p_c, and then we characterize the transmission probability of STs.

The minimum power harvested by a ST in one slot is $\eta P_p r_h^{-\alpha}$, which occurs when the ST is at the edge of a harvesting zone. Therefore, the battery of an energy-harvesting ST can be charged to the transmission threshold within one slot time if $0 < \beta P_s \leq \eta P_p r_h^{-\alpha}$, thus this case is referred to as *single-slot charging*. Similarly, if $\eta P_p r_h^{-\alpha} < \beta P_s \leq 2\eta P_p r_h^{-\alpha}$, a ST needs at most two slots of harvesting to reach the transmission threshold, which is called *double-slot charging*. In either case, the battery power level can be exactly modeled by a finite-state Markov chain (MC), and the transmission probability p_t can be obtained accordingly. Otherwise, if $\beta P_s > 2\eta P_p r_h^{-\alpha}$, a ST needs at most N ($N > 2$) slots of harvesting to reach the transmission threshold, i.e., *multi-slot charging*. In this case, we can only obtain upper and lower bounds on p_t by using MC theory. However, since small value of P_s is of our interest, we will analyze the transmission probability in two different conditions as follows.

3.1 Single-Slot Charging

If $0 < \beta P_s \leq \eta P_p r_h^{-\alpha}$, i.e., $0 < \beta \leq \frac{\eta P_p r_h^{-\alpha}}{P_s}$, the battery is charged to the transmission threshold within one slot. Thus the power level can be characterized as two states $\{0, 1\}$, which are mapped to the power level 0 and the range $[\beta P_s, P_s]$, respectively. Accordingly, the state transition probability matrix denoted as $\mathbf{P}_1$ is obtained as

$$\mathbf{P}_1 = \begin{bmatrix} 1 - p_h & p_h \\ p_g & 1 - p_g \end{bmatrix}. \tag{4}$$

Therefore, we have the following proposition.

Proposition 1. *If* $0 < \beta \leq \frac{\eta P_p r_h^{-\alpha}}{P_s}$, *the transmission probability of a typical ST is obtained as*

$$p_t = p_c p_g = \frac{p_h}{p_h + p_g} p_g. \tag{5}$$

Proof. The probability p_c can be obtained by solving $\boldsymbol{\pi_1} = \boldsymbol{\pi}_1 \mathbf{P}_1$, where $\boldsymbol{\pi_1}$ is the steady-state probability vector given by $\boldsymbol{\pi_1} = \left[\boldsymbol{\pi_1^0}, \boldsymbol{\pi_1^1}\right]$. In this case, $p_c = \boldsymbol{\pi_1^1}$. This completes the proof of Proposition 1.

From (5), it is observed that the transmit probability of a ST has no dependence on β. This is because once a ST lies in the harvesting zone, it is guaranteed to be charged to the threshold within one slot as the proposed condition $0 < \beta P_s \leq \eta P_p r_h^{-\alpha}$.

3.2 Double-Slot Charging

If $\eta P_p r_h^{-\alpha} < \beta P_s \leq 2\eta P_p r_h^{-\alpha}$, i.e., $\frac{1}{P_s}\eta P_p r_h^{-\alpha} < \beta \leq \frac{2}{P_s}\eta P_p r_h^{-\alpha}$, the battery of the ST needs at most two slots to reach the transmission threshold. We divide the harvesting zone into two parts as shown in Fig. 1, where T_p denotes a typical PT, a disk centered at T_p with radius h_1 denotes $\mathcal{H}_1$, and an annulus centered at T_p with radii $0 < h_1 < r_h$ denotes $\mathcal{H}_2$, and h_1 and r_h are the inner and outer

diameter of the annulus, respectively. We can derive h_1 as $h_1 = \left(\frac{\beta P_s}{\eta P_p}\right)^{-\frac{1}{\alpha}}$. We consider T_s as a typical ST, and the average energy harvested by the T_s from T_p in one slot is $\eta P_p D^{-\alpha}$. If T_s is located inside the region $\mathcal{H}_1$, it will be charge to the range $[\beta P_s, P_s]$, else if T_s is located in the region $\mathcal{H}_2$, the power harvested is in the range $\left[\frac{1}{2}\beta P_s, \beta P_s\right)$.

Let us consider a three state MC with state space $\{0, 1, 2\}$, since $\eta P_p r_h^{-\alpha} \geq \frac{1}{2}\beta P_s$. In this case, the battery power level can be 0, in the range $\left[\frac{1}{2}\beta P_s, \beta P_s\right)$, or in the range $[\beta P_s, P_s]$, which are mapped to the states 0, 1, and 2, respectively. From Fig. 1, the state transition probability matrix denoted by $\mathbf{P}_2$ can be obtained as

$$\mathbf{P}_2 = \begin{bmatrix} 1-p_h & p_h - p_1 & p_1 \\ 0 & 1-p_h & p_h \\ p_g & 0 & 1-p_g \end{bmatrix}. \tag{6}$$

Similarly to (1), the probability of $p_1 = \Pr\{T_s \in \mathcal{H}_1\}$ is obtained as $p_1 = 1 - e^{-\pi h_1^2 \mu_p}$. Based on the above analysis, we have the following proposition.

Proposition 2. *If* $\frac{1}{P_s}\eta P_p r_h^{-\alpha} < \beta \leq \frac{2}{P_s}\eta P_p r_h^{-\alpha}$, *the transmission probability of a typical ST is obtained as*

$$p_t = p_c p_g = \frac{p_h}{p_h + p_g\left(\frac{2p_h - p_1}{p_h}\right)} p_g. \tag{7}$$

Proof. The result in (7) can be obtained similarly as Proposition 1, i.e., by solving $\boldsymbol{\pi_2} = \boldsymbol{\pi_2}\mathbf{P}_2$, where $\boldsymbol{\pi_2}$ is the steady-state probability vector given by $\boldsymbol{\pi_2} = \left[\boldsymbol{\pi_2^0}, \boldsymbol{\pi_2^1}, \boldsymbol{\pi_2^2}\right]$, and we obtain $p_c = \boldsymbol{\pi_2^2}$. This completes the proof of Proposition 2.

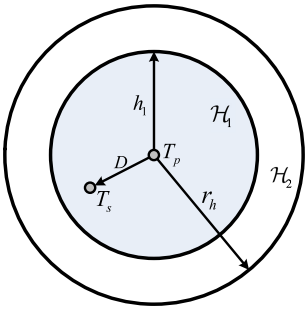

Fig. 1. The partitioned harvesting zone of double-slot charging.

Note that from (7), we can easily obtain that p_t is a decreasing function of β. An intuitive explanation of the above observation is that, if β grows, the time required for battery charging will get longer, thus leading to a lower p_t.

4 Coverage Probability

In this section, the coverage probabilities of the primary network and the secondary network are investigated. Note that due to the energy-based OSA, the point process developed by active STs does not follow a HPPP, and is difficult to characterize accurately. To simplify our analysis, following the assumptions in [5], we assume that the point process of active STs follows a HPPP, which will be verified by our simulation results. Let Φ_a denote the point process of active STs, I_p and I_s denote the aggregate interference at the origin from all PTs and active STs, respectively, which are modeled by *shot-noise processes* [6], given by

$$I_p = \sum_{X \in \Phi_p} h_X P_p |X|^{-\alpha}, \tag{8}$$

$$I_s = \sum_{Y \in \Phi_a} h_Y \overline{P}_s |Y|^{-\alpha}, \tag{9}$$

where $|X|, |Y|$ denote the distances from node X, Y to the origin, respectively, and $\{h_X\}$ and $\{h_Y\}$ are independent and identically distributed (i.i.d.) exponential random variables with unit mean. $\overline{P}_s$ denotes the average power of all the transmitting STs. Since the transmit power of the active STs are kept in a range $[\beta P_s, P_s]$, we have $\beta P_s < \overline{P}_s < P_s$. Intuitively, $\overline{P}_s$ is increasing with β. Similar to [4], we make the following approximations on the conditional distribution of the active STs, which will be verified by simulations in Section 6.

Assumption 1. *The point process formed by the active STs Φ_a follows a HPPP with density $p_t \mu_s$.*

4.1 Primary Network

To analyze the coverage probability of the primary network, we concentrate on a typical PR at the origin denoted by R_p with its intended PT denoted as T_p at a distance of d_p away. By using Slivnyak's theorem [7], in this case, the locations of the rest of the active PRs and PTs are both HPPPs with density μ_p. Therefore, the coverage probability of the primary network τ_p is given by

$$\tau_p = \Pr\{SIR_p \geq \theta_p\} = \Pr\left\{\frac{h_p P_p d_p^{-\alpha}}{I_p + I_s} \geq \theta_p\right\}, \tag{10}$$

where h_p is the channel power between R_p and its intended T_p. Then we have the following theorem.

Theorem 1. *Under Assumption 1, the average coverage probability of the primary network $\overline{\tau}_p$ is given by*

$$\overline{\tau}_p = \exp\left(-\left(\theta_p^{\frac{2}{\alpha}} d_p^2 \varphi \left(p_t \mu_s \left(\frac{\overline{P}_s}{P_p}\right)^{\frac{2}{\alpha}} + \mu_p\right)\right)\right), \tag{11}$$

where $\varphi = \pi \Gamma\left(1 + \frac{2}{\alpha}\right) \Gamma\left(1 - \frac{2}{\alpha}\right)$, and $\alpha > 2$ with $\Gamma(x) = \int_0^\infty t^{x-1} e^{-t} dt$ indicating the Gamma function.

Proof. The proof is omitted due to the space limitation. Please refer to [4].

Corollary 1. *Under Assumption 1 and the analysis above. the coverage probability of the primary network is upper-bounded and lower-bounded, respectively, by,*

$$\tau_p < \exp\left(-\left(\theta_p^{\frac{2}{\alpha}} d_p^2 \varphi \left(p_t \mu_s \left(\frac{\beta P_s}{P_p}\right)^{\frac{2}{\alpha}} + \mu_p\right)\right)\right), \tag{12}$$

$$\tau_p > \exp\left(-\left(\theta_p^{\frac{2}{\alpha}} d_p^2 \varphi \left(p_t \mu_s \left(\frac{P_s}{P_p}\right)^{\frac{2}{\alpha}} + \mu_p\right)\right)\right). \tag{13}$$

Proof. From (11), it can be observed that τ_p is a function of p_t and $\overline{P}_s$. An intuitive explanation of the above observation is that $\beta P_s < \overline{P}_s < P_s$. However, from Section 3, p_t is a constant for a given transmission threshold βP_s. Thus we can obtain (12) and (13) by substituting $\beta P_s < \overline{P}_s < P_s$ into (11).

4.2 Secondary Network

Under Assumption 1, to analyze the coverage probability of the secondary network, we concentrate on a typical SR at the origin denoted by R_s with its intended ST denoted as T_s at a distance of d_s away. By using Slivnyak's theorem, in this case, the locations of the rest of the active SRs and STs both follow HPPPs with density $p_t\mu_s$.

Since the STs cannot transmit if they are inside any guard zone of the PTs, to approximate τ_s, we consider the coverage probability conditioned on T_s being outside all the guard zones which means that there is no PT inside the disk centered at T_s with radius r_g, denoted as $\mathcal{G}_{T_s}^{r_g}$. Let the condition discussed above be denoted by $\zeta = \{\Phi_p \cap \mathcal{G}_{T_s}^{r_g} = \emptyset\}$. Then the coverage probability of the secondary network is given by

$$\tau_s = \Pr\left\{\frac{h_s P_{T_s} d_s^{-\alpha}}{I_p + I_s} \geq \theta_s \,|\zeta\right\}, \tag{14}$$

where h_s is the channel power between R_s and its intended T_s, P_{T_s} is the transmit power of the intended T_s, and $\beta P_s \leq P_{T_s} \leq P_s$. The active STs follow a HPPP with density $p_t\mu_s$ which means that none of the active STs are inside a guard zone, that is, $\Pr\{\zeta\} = 1$. Moreover, under the assumption $P_p \gg P_s$, it is a reasonable assumption that the interference from every PT inside $\mathcal{G}_{T_s}^{r_g}$ will cause an outage to the typical R_s at the origin. Thus, we have $\Pr\left\{h_s \geq \frac{\theta_s d_s^{\alpha}}{P_{T_s}} (I_p + I_s) \,|\bar{\zeta}\right\} \approx 0$. Then we have the following theorem.

Theorem 2. *Under Assumption 1, the average coverage probability of the secondary network $\overline{\tau}_s$ is obtained as*

$$\overline{\tau}_s = \exp\left(-\left(p_t\mu_s + \mu_p \left(\frac{\overline{P}_s}{P_p}\right)^{-\frac{2}{\alpha}}\right)\theta_s^{\frac{2}{\alpha}} d_s^2 \varphi\right). \tag{15}$$

Proof. The proof is omitted due to the space limitation.

Corollary 2. *Under Assumption 1 and the analysis above. The coverage probability of the secondary network is upper-bounded and lower-bounded, respectively, by,*

$$\tau_s < \exp\left(-\left(p_t\mu_s + \mu_p\left(\frac{P_s}{P_p}\right)^{-\frac{2}{\alpha}}\right)\theta_s^{\frac{2}{\alpha}} d_s^2\varphi\right), \tag{16}$$

$$\tau_s > \exp\left(-\left(p_t\mu_s + \mu_p\left(\frac{\beta P_s}{P_p}\right)^{-\frac{2}{\alpha}}\right)\theta_s^{\frac{2}{\alpha}} d_s^2\varphi\right). \tag{17}$$

Proof. This can be proved by applying a similar approach as used for the proof of Corollary 1.

5 Network Throughput

5.1 Primary Network

We characterize the throughput of the primary network as $C_p = \mu_p\tau_p \log(1+\theta_p)$. Note that the primary network throughput C_p mainly reflects the coverage probability τ_p. With (12) and (13), the throughput of the primary network is upper-bounded and lower-bounded, respectively, by,

$$C_p < \mu_p \log(1+\theta_p) \times \exp\left(-\left(\theta_p^{\frac{2}{\alpha}} d_p^2\varphi\left(p_t\mu_s\left(\frac{\beta P_s}{P_p}\right)^{\frac{2}{\alpha}} + \mu_p\right)\right)\right), \tag{18}$$

$$C_p > \mu_p \log(1+\theta_p) \times \exp\left(-\left(\theta_p^{\frac{2}{\alpha}} d_p^2\varphi\left(p_t\mu_s\left(\frac{P_s}{P_p}\right)^{\frac{2}{\alpha}} + \mu_p\right)\right)\right). \tag{19}$$

5.2 Secondary Network

We characterize the throughput of the secondary network as $C_s = \mu_s p_t \tau_s \log(1+\theta_s)$. The throughput of the secondary network C_s is a function of both p_t and τ_s. However, from Section 3, p_t is a constant for a given transmission threshold βP_s. Therefore, C_s is only dependent on τ_s. From (16) and (17), the throughput of the secondary network is upper-bounded and lower-bounded, respectively, by

$$C_s < \mu_s \log(1+\theta_s)\, p_t \times \exp\left(-\left(p_t\mu_s + \mu_p\left(\frac{P_s}{P_p}\right)^{-\frac{2}{\alpha}}\right)\theta_s^{\frac{2}{\alpha}} d_s^2\varphi\right), \tag{20}$$

$$C_s > \mu_s \log(1+\theta_s)\, p_t \times \exp\left(-\left(p_t\mu_s + \mu_p\left(\frac{\beta P_s}{P_p}\right)^{-\frac{2}{\alpha}}\right)\theta_s^{\frac{2}{\alpha}} d_s^2\varphi\right). \tag{21}$$

Remark 1: The maximum throughput of the secondary network is obtained with the transmission threshold coefficient $\beta^* = \frac{1}{P_s}\eta P_p r_h^{-\alpha}$, which will be verified by simulation in Section 6 by Fig. 3(b). Note that $\beta^* = \frac{1}{P_s}\eta P_p r_h^{-\alpha}$ can be write as $\beta^* P_s = \eta P_p r_h^{-\alpha}$, where $\beta^* P_s$ is exactly the transmission threshold. As mentioned in Section 3, the minimum power harvested by a ST in one slot is $\eta P_p r_h^{-\alpha}$, which means that, the secondary network throughputs are maximized over the energy-based OSA strategy if each candidate ST's harvested energy within one slot is larger than the transmission threshold.

6 Numerical Result

In this section, based on our theoretical analysis, we provide some numerical results and give some interpretations. Unless otherwise specified, we set the harvesting efficiency as $\eta = 0.1$ and the path-loss exponent as $\alpha = 4$.

Fig. 2(a) and Fig. 2(b) show the ST transmission probability p_t versus the ST transmission threshold coefficient β and the ST maximum transmit power P_s, respectively. From Fig. 2(a), it is observed that p_t is consistent with our analysis in Section 3. Furthermore, both Fig. 2(a) and Fig. 2(b) show that the transmit probability with $0 < \beta < 1$ outperforms the transmit probability with $\beta = 1$, which means that the performance of the energy-based OSA strategy outperforms that of the scheme in [4], since $\beta = 1$ means that the batteries of STs are fully charged.

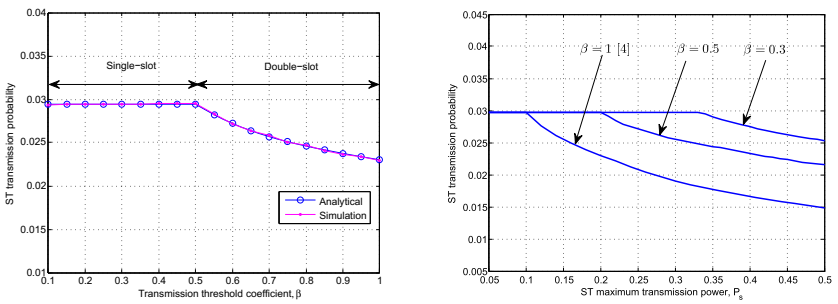

(a) (b)

Fig. 2. (a) The ST transmission probability p_t versus the ST transmission threshold coefficient β; (b) The ST transmission probability p_t versus the ST maximum transmission power P_s.

In Fig. 3(a), we compare the analytical and simulated results on the coverage probability using the energy-based OSA scheme. We have following observations. First, the simulation results fall between the upper bounds and the lower bounds as expected, thus Assumption 1 is validated. Second, the coverage probability of the primary network τ_p is insensitive to β, this can be explained from (10), since

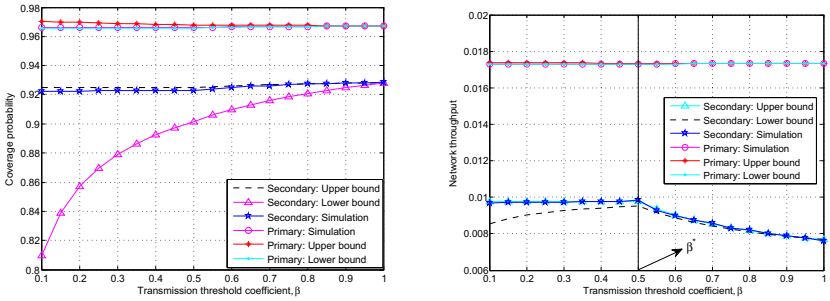

(a) (b)

Fig. 3. (a) The network coverage probability versus the ST transmission threshold coefficient β; (b) The network throughput versus the ST transmission threshold coefficient β.

larger β increases the interference level from active STs (resulting in smaller τ_p) but at the same time reduces the ST transmission probability p_t and thus resulting in larger τ_p. Third, the coverage probability of the secondary network τ_s grows slightly with β, which can be explained theoretically from our result in (15), the numerator and the aggregate interference I_s in the denominator are both increasing with β, but the increment of I_s is negligible compared to I_p according to the condition $P_s \ll P_p$ and thus can be ignored. That is to say, compared with the scheme in [4], the coverage probabilities using energy-based OSA strategy are not changed significantly.

In Fig. 3(b), we compare the analytical and simulated results for the network throughput under the energy-based OSA scheme. Several observations follow. First, it is also observed that the simulated throughputs fall between the upper bounds and the lower bounds as expected. Second, the throughput of the primary network C_p is insensitive to β. This is because C_p mainly depends on τ_p and we have mentioned that τ_p is insensitive to β. Third, we show the maximum throughput of the secondary network is obtained with the transmission threshold coefficient $\beta^* = \frac{1}{P_s}\eta P_p r_h^{-\alpha}$. This can be explained as follows. On one hand, if $0 < \beta \leq \beta^*$, it can be observed that the transmit probability p_t is a constant, thus C_s depends only on τ_s. From the analysis above, τ_s grows slightly with β, therefore, C_s is increasing with β slightly. On the other hand, if $\beta > \beta^*$, C_s is dependent on both p_t and τ_s. However, p_t affects C_s more significantly than τ_s, and p_t is decreasing with β, which indicates that C_s is decreasing with β. Fourth, the network throughput with $0 < \beta < 1$ outperforms the throughput with $\beta = 1$, as much as 29% at $\beta^* = \frac{1}{P_s}\eta P_p r_h^{-\alpha}$, which confirms that the performance of the energy-based OSA strategy outperforms that of the scheme in [4].

7 Conclusion

In this paper, we proposed a VP transmission mode and an energy-based OSA strategy for opportunistic energy harvesting in CR networks. Using tools from

stochastic geometry, the transmission probability of the STs considering the influence of both the guard zones and harvesting zones was derived. Moreover, we investigated the coverage probabilities and network throughputs of the primary and the secondary networks, respectively. Theoretical analysis and simulation results show that, compared with previous work, the transmission probability and the throughput of the secondary network with the energy-based OSA strategy are both significantly improved. The throughput is increased by as much as 29%. It is hoped that the results in this paper could provide new insights to the optimal design of other wireless powered communication networks.

References

1. Visser, H.J., Vullers, R.J.M.: RF Energy Harvesting and Transport for Wireless Sensor Network Applications: Principles and Requirements. Proc. IEEE **101**, 1410–1423 (2013)
2. Kingman, J.F.C.: Poisson Processes. Oxford University Press (1993)
3. Dhillon, H., Li, Y., Nuggehalli, P., Pi, Z., Andrews, J.: Fundamentals of Heterogeneous Cellular Networks with Energy Harvesting. IEEE Trans. Wireless Commun. **13**, 2782–2797 (2014)
4. Lee, S., Zhang, R., Huang, K.: Opportunistic Wireless Energy Harvesting in Cognitive Radio Networks. IEEE Trans. Wireless Commun. **12**, 4788–4799 (2013)
5. Song, X., Yin, C., Liu, D., Zhang, R.: Spatial Throughput Characterization in Cognitive Radio Networks with Threshold-Based Opportunistic Spectrum Access. IEEE J. Sel. Areas Commun. **32**, 2190–2204 (2014)
6. Haenggi, M., Ganti, R.K.: Interference in Large Wireless Networks. Found. Trends in Netw., 127–248 (2008)
7. Haenggi, M., Andrews, J., Baccelli, F., Dousse, O., Franceschetti, M.: Stochastic Geometry and Random Graphs for the Analysis and Design of Wireless Networks. IEEE J. Sel. Areas Commun. **27**, 1029–1046 (2009)